# Performance analysis of AO-OFDM-CDMA with advanced 2D-hybrid coding for amplifier-free LR-PONs

Hichem Mrabet, Sofien Mhatli, Iyad Dayoub, Elias Giacoumidis

IET Optoelectronics

Research Article

IET Journals
The Institution of Engineering and Technology

# Performance analysis of AO-OFDM-CDMA with advanced 2D-hybrid coding for amplifier-free LR-PONs

ISSN 1751-8768
Received on 4th September 2017
Revised 15th May 2018
Accepted on 9th July 2018
E-First on 29th August 2018
doi: 10.1049/iet-opt.2018.5042
www.ietdl.org

*Hichem Mrabet*[1,2] ✉, *Sofien Mhatli*[2], *Iyad Dayoub*[3], *Elias Giacoumidis*[4]

[1]*IT Department, College of Computation and Informatics, Saudi Electronic University, Medina Branch, Kingdom of Saudi Arabia*
[2]*SERCOM-Lab, Tunisia Polytechnic School, Carthage University, 2078 La Marsa, Tunis, Tunisia*
[3]*University of Valenciennes, CNRS, University of Lille, YNCREA, Centrale Lille, UMR 8520 – IEMN, DOAE, Valenciennes F-59313, France*
[4]*School of Electronic Engineering, Dublin City University, Radio and Optical Communications Laboratory, Dublin 9, Ireland*
✉ *E-mail: h.mrabet@seu.edu.sa*

**Abstract:** All-optical orthogonal frequency division multiplexing (AO-OFDM) and optical code-division multiple-access system (OCDMA) are combined in the first analytical model, which considers subcarrier hopping by means of advanced two-dimensional (2D) hybrid-coded (2D-HC) signature. The model incorporates probabilistic subcarrier overlapping, multiple-access interferences and is tested, for the first time, over amplifier-free long-reach passive optical networks (LR-PONs) using cost-effective intensity modulations and direct detection. For the upstream direction at 40 Gb/s, AO-OFDM-OCDMA outperforms a 'classical' multi-channel OCDMA system for low received powers and any number of simultaneous users. In comparison to conventional 1D Walsh–Hadamard, 1D prime code and 2D prime hop system, coding with 2D-HC can improve the performance of AO-OFDM-CDMA, thus allowing a higher number of simultaneous users in LR-PON without optical amplification. From numerical simulations, the authors show that 16-quadrature amplitude modulation (16-QAM) AO-OFDM-CDMA with 45 users has comparable performance to conventional multi-channel 16-QAM coherent optical OFDM in the downstream direction and up to 58 km with 1:45 split ratio, without employing complex coherent technology. Similarly, based on the feasibility of physical implementation configuration, a budget power calculation is performed showing 108 km as maximum reachability distance for 40 Gb/s QAM signal, 1:64 split ratio when considering standard forward-error-correction.

## 1 Introduction

The effectiveness of broadband access networks can be further improved in order to satisfy the increasing demand for users in terms of throughput, quality of service and security. In the state-of-the-art, various broadband access technologies have been introduced which include classical wired digital subscriber line networks, hybrid fibre coax network for cable modem customers, wireless networks using satellite communications, optical carrier level-*n*, synchronous transfer system level-*n* for business customers and passive optical networks (PONs) for ultra-high-bandwidth applications [1].

Nowadays, a PON is one of the most important next-generation access networks that is proliferating due to its cost and energy efficiency by employing passive components between end users and operators. The importance of the employment of PONs in access has led to the following standardised solutions: ITU-T G.983, IEEE 802.3ah, ITU-T G.987 and ITU-T G.989.1 for broadband PON [2], Ethernet PON [3, 4] 10 Gb PON [5] and NG-PON2 [6]. However, in order to increase the distance between the user and central offices, thus providing a long-reach PON (LR-PON) configuration, optical amplification is considered the only valuable solution which unfortunately adds cost and energy consumption, while forbidding the practical implementation of a 'pure PON' [7, 8]. Then again, to meet the exponential customer demand in PON access network and to exploit the higher capacity provided by the fibre link, several multiplexing techniques have been proposed for PONs such as time-division multiplexing (DM), wavelength DM (WDM) [9], orthogonal frequency DM (OFDM) [10] and optical code DM (OCDM) [11].

OCDM for access [i.e. optical code-division multiple-access system (OCDMA)] has been employed to permit all users to share the same transmission media (time, wavelength) but for each of them, a unique optical code is assigned, according to which the proper optical decoder can distinguish different users at the receiver [12]. Owing to the all-optical (AO) processing-based code generation and recognition, OCDMA exhibits the unique features of allowing fully asynchronous transmission, low-latency access which is desirable for burst traffic environment, protocol transparency, high network flexibility, simplified network management and so on [13]. Among all the other potential advantages, providing the information security is generally considered as an inherent benefit of OCDMA [13]. On the other hand, AO-OFDM [7] in a new type of advanced multi-carrier modulation technique that tends to provide, almost always, a one-step higher data rate in a transmission system than a state-of-the-art electronic system. The electronic fast Fourier transform (FFT) and OFDM symbol modulation can be replaced by an AO discrete Fourier transform to overcome the electronics speed limit.

In this work, we propose the first hybrid AO-OFDM-CDMA system and theoretically analyse its performance on amplifier-free LR-PONs, harnessing higher-order modulation formats and using cost-effective intensity modulation and direct detection (IM/DD). A novel analytical model is employed which combines a probabilistic approach of optical subcarrier overlapping and hopping using advanced two-dimensional hybrid-coded (2D-HC) signature, taking into account multiple-access interferences (MAI) and receiver beat noise [12]. To the best of knowledge, this is the first theoretical analysis of such hybrid model in amplifier-free IM/DD LR-PONs, thus providing a guideline for the future practical implementation of AO-OFDM-CDMA to enable users' capacity enhancement, improved spectral efficiency and security cost-effectively. In our previous work reported in [14], we presented a numerical performance analysis of a hybrid electronic-based OFDM-OCDMA system using IM/DD and a prime hop system (PHS) CDMA coding by taking into account only the MAI and photodetector noise over 80 km of fibre length. Here, we present for the first time, an AO configuration for OFDM-CDMA (namely AO-OFDM-CDMA) system with direct detection by means of more advanced 2D-HC-CDMA coding for multiplexing schema. Also in this paper, for the first time we perform a simulation comparison of AO-OFDM-CDMA with a conventional

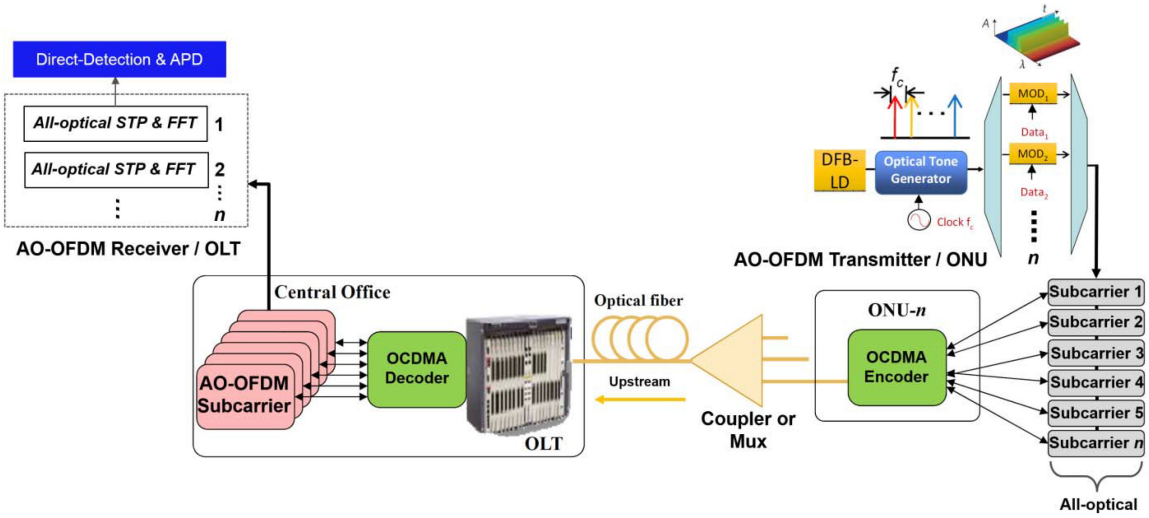


**Fig. 1** *Proposed hybrid AO-OFDM-CDMA architecture for amplifier-free LR-PON with DD*

APD: avalanche photodiode; STP: serial-to-parallel; FFT: fast Fourier transforms; *n*: *n*-user; OLT: optical line terminal; Mux: multiplexer; ONU: optical network unit; DFB: distributed-feedback laser; MOD: modulator

WDM-CO-OFDM including MAI, subcarriers overlap, linear and non-linear effects at 40 Gb/s and 45 users. A second comparison is also made in this paper, showing that the AO-OFDM-CDMA using 2D-HC outperforms both 2D-PHS [14] and 1D Walsh–Hadamard [15] CDMA coding in terms of bit-error rate (BER).

## 2 System architecture

Fig. 1 depicts the physical implementation of the proposed AO-OFDM-CDMA system for amplifier-free LR-PON configuration. The system architecture includes the optical line terminal (OLT), the transmission channel, the power splitter and the optical network unit (ONU). A distributed-feedback laser (DFB-LD) is launched into an 'Optical Tone Generator', which is consisted of a cascaded phase modulators electrically. Multiple phase-locked optical tones (optical comb) with a frequency separation of 5 GHz is produced. Then the optical tones are wavelength de-multiplexed and encoded with 40 to 160 Gb/s signals employing different level-orders of the quadrature amplitude modulation (QAM) with proper delay via the optical modulators (MODs). Then different modulated optical tones are combined and transmitted through standard single-mode fibre (SSMF). A distinct number of sub-channels (i.e. a group of optical subcarriers) are combined by a splitter (downstream)/coupler (upstream) or an array waveguide grating (AWG). At the OLT, after special coding with OCDMA on each optical subcarrier the serialised AO-OFDM system is converted into parallel streams, and subsequently, an optical FFT unravels the optical subcarriers for DD using an avalanche photodiode (APD) and single-carrier demodulation [8].

## 3 System model

The AO-OFDM-CDMA analytical model incorporates the encoder (i.e. ONU), the channel and the decoder system (i.e. OLT).

### 3.1 ONU model

At the OFDM modulation block output, the generated AO-OFDM symbols, $S_m$, at a centre frequency $f_c$ is given by

$$S_m(t) = \frac{1}{\sqrt{N}} \sum_{k=1}^{N} X_k \exp\left(\frac{j2\pi f_c t}{N}\right) \quad (1)$$

where $N$ is the size of aggregated optical orthogonal subcarriers (i.e. packet size) and $X_k$ are the total input symbols.

At the $k$th user encoder end, the signal can be described by the following expression:

$$s_k(t) = \sum_{i=0}^{F-1} P_T S_m(t) c_k(t - iT_c) \quad (2)$$

where $P_T$, $c_k$ and $F$ are the launched optical power (LOP), the $k$th OCDMA signature and the code length, respectively. For the OCDMA, the optical code of the $k$th user is known as a code signature $c_k(t)$ and is expressed by [16]

$$c_k(t) = \sum_{i=1}^{F} d_{k,i} P(t - iT_c) \quad (3)$$

where $P(t - iT_c)$ is a unit rectangular pulse of duration $T_c$ (chip duration) and $d_{k,i} \in \{0, 1\}$ is the $i$th value of the $k$th user signature. Afterwards, we implement an advanced 2D-HC signature in which a maximum likelihood sequence is processed for the optical subcarrier hopping (GHz spacing sub-wavelengths), while the prime number is used for temporal spreading and set to 31 [16]. For instance, a hybrid code sequence using the numbers {1, 2, 3, 4, 5, 6, 7} symbolising the wavelength $\{\lambda_1, \lambda_2, \lambda_3, \lambda_4, \lambda_5, \lambda_6, \lambda_7\}$ is illustrated in Table 1.

In fact, the number of active users in the OCDMA system depends on the OCDMA code parameters (i.e. the prime number $P$) [17]. At a given $P$, the OCDMA system can support $P(P+1)$ users for 2D-HC. When $P$ is equal to 31, the maximum theoretical number of users considering only MAI is equal to $31 \times 32$, leading to 992 users for 2D-HC.

Table 2 provides the theoretical number of users with conventional correlation receiver (CCR) and with serial interference cancellation (SIC) at a BER of $10^{-9}$ for 1D prime code (1D-PC), 2D-PHS codes and 2D-HC with $P$ equal to 31, respectively.

Owing to the attractive features of 2D-HC which include higher user capacity and enhanced spectral efficiency, such codes are selected in the adopted AO-OFDM-OCDMA.

At the inverse FFT output, the total signal can be described by

$$S(t) = \sum_{k=1}^{K} s_k(t) \exp(j2\pi f_o t) \quad (4)$$

where $K$ is the number of network subscribers (i.e. users) and $f_o$ is the central frequency at 1550 nm.

### 3.2 Channel model

The channel model architecture comprises a power splitter, the optical fibre which is based on SSMF and a block loop to fulfil the user requirements for different link lengths. The adopted LOP for

both hybrid AO-OFDM-CDMA and a 'classical' OCDMA [12] for reference measurement was set at 10 dBm to enable longer PON-length transmission. To compensate the SMF-induced chromatic (CD) effects, a CD compensating fibre was employed with a negative CD coefficient ($-\mathrm{CD_c} \times$ length). It should be noted that fibre non-linearities are out of the scope of this paper and will be addressed in future work.

### 3.3 OLT model

As depicted in Fig. 1, the OLT decoder model architecture is composed of the APD, the demodulator per optical subcarrier (single-carrier demodulation) and an AWG decoder. At the output of the AWG decoder, the estimated symbol $\hat{s}_k(t)$ is provided to the OLT. At the receiver, the photodetector output, $Z_i(t)$, is defined as follows [18]:

$$Z_i(t) = \frac{RP_{\mathrm{R}}}{2}\int_0^{T_{\mathrm{b}}} \sum_{k=1}^{K}\sum_{l=0}^{N-1} S_m(t)C_k(t - lT_{\mathrm{c}})\,\mathrm{d}t + \phi \tag{5}$$

where $R$, PR, $T_{\mathrm{b}}$ and $\phi$ are the receiver responsivity (0.9 A/W), the optical received power, the bit period and the APD beat noise (shot and thermal noises) with parameters identical to [12]. The received optical power is related to the LOP as follows:

$$P_{\mathrm{R}} = P_{\mathrm{T}} - \alpha L \tag{6}$$

in which $\alpha$ and $L$ are the attenuation coefficient and the SMF length, respectively.

## 4 System performance metrics

The optical signal-to-noise ratio (SNR) as a function of simultaneous PON users (i.e. $K$) is expressed by

$$\mathrm{SNR} = \frac{S}{(K-1)\sigma^2 + N_0} \tag{7}$$

where $S$ is the received signal, $\sigma^2$ is the noise variance and $N_0$ is the photodetector noise. $S$ is related to the photodetector current ($I$) by $S = I^2$ and

$$I = \frac{\mathrm{GRP_R}}{\mathrm{MF}} \tag{8}$$

where $G$ is the gain set at 15 dB and multiplication factor (MF) is the 'MF' of APD [12].

The noise variance $N_0$ is the addition of the thermal noise ($N_{\mathrm{th}}$) and the photodetector shot noise power ($N_{\mathrm{sh}}$) is given by [16]

$$N_{\mathrm{th}} = \frac{4K_{\mathrm{B}}T}{R_{\mathrm{l}}}\Delta F \tag{9}$$

where $K_{\mathrm{B}}$ is the Boltzmann constant, $T$ and $R_{\mathrm{l}}$ are the receiver equivalent temperature and the load charge resistance, respectively. In addition, $\Delta F$ is the electrical photodetector bandwidth for each optical subcarrier. $N_{\mathrm{sh}}$ is given by [19]

$$N_{\mathrm{sh}} = \frac{2qR_{\mathrm{l}}K_{\mathrm{B}}P_{\mathrm{R}}}{4T} \tag{10}$$

where $q$ is the electron charge. In our proposed model, the noise variance includes MAI and overlap of AO-OFDM subcarriers which is defined as follows:

$$\sigma^2 = \sigma^2_{\mathrm{MAI}} + \sigma^2_{\mathrm{overlap}} \tag{11}$$

In (12), where $\sigma^2_{\mathrm{MAI}}$ is related to 2D-HC defined by [16]

$$\sigma^2_{\mathrm{MAI}} = \frac{H}{2P^2}\left(1 - \frac{H}{2P^2}\right) \tag{12}$$

where $H$ and $P$ are the average probability hit of chips related to 2D-HC and the prime number, respectively. For our system analysis, we estimate the BER derived from (8) as follows:

$$\mathrm{BER} = \frac{2}{\log_2(M)}\left(1 - \frac{1}{\sqrt{M}}\right)\mathrm{erfc}\left(\sqrt{\frac{3\mathrm{SNR}}{2(M-1)}}\right) \tag{13}$$

where $M$ is the modulation format level. Finally, a Q-factor in dB is deduced from BER in (13) by

$$Q_{\mathrm{dB}} = 20\log_{10}\left(\sqrt{2}\mathrm{erfc}^{-1}(2\mathrm{BER})\right) \tag{14}$$

## 5 Simulated analysis for upstream LR-PON

To maximise bit rates, we harness QAM-order modulation format ($M$) for each optical subcarrier ($N_{\mathrm{s}}$) thus providing bit rates per $N_{\mathrm{s}}$ of 40 Gb/s and up to 160 Gb/s. Table 3 exhibits the simulation parameters deployed for the numerical results of SNR, BER and Q-factor calculations, in particular for DFB transmitter, SSMF specification G.652 [20], APD specification [21] and CDMA code properties, respectively.

Fig. 2 shows the SNR evolution as a function of PR for various $N_{\mathrm{s}}$ ranging from 64 to 256.

As depicted in Fig. 2, the SNR of AO-OFDM-OCDMA system at 20 km upstream LR-PON is slightly enhanced at high PR and $N_{\mathrm{s}}$. This occurs because the SNR is increased for a high $N_{\mathrm{s}}$ resulting in the low variance of optical subcarrier overlapping.

Fig. 3 presents the log(BER) evolution as a function of PR for AO-OFDM-CDMA when employing a different order of

**Table 1** Seven 2D-HC sequences with $P = 7$

| | | | | | | | |
|---|---|---|---|---|---|---|---|
| $S_0H_1$ | 30000000 | 20000000 | 70000000 | 00000000 | 00000000 | 10000000 | 00000000 |
| $S_2H_1$ | 50000000 | 40000000 | 20000000 | 00000000 | 00000000 | 30000000 | 00000000 |
| $S_4H_1$ | 20000000 | 10000000 | 60000000 | 00000000 | 00000000 | 70000000 | 00000000 |
| $S_1H_2$ | 10000000 | 70000000 | 50000000 | 00000000 | 00000000 | 60000000 | 00000000 |
| $S_3H_2$ | 40000000 | 30000000 | 10000000 | 00000000 | 00000000 | 20000000 | 00000000 |
| $S_0H_3$ | 60000000 | 50000000 | 30000000 | 00000000 | 00000000 | 40000000 | 00000000 |
| $S_2H_3$ | 70000000 | 60000000 | 40000000 | 00000000 | 00000000 | 50000000 | 00000000 |

**Table 2** Number of users for different OCDMA codes with $P = 31$

| OCDMA codes | Theoretical number of users | Number of users with CCR receiver | Number of users with SIC receiver |
|---|---|---|---|
| 1D-PC | 31 | 25 | 30 |
| 2D-PHS | 930 | 200 | 500 |
| 2D-HC | 992 | 520 | 961 |

**Table 3** Simulation parameters

| Parameter | Value |
|---|---|
| central wavelength | 1550 nm |
| modulation format per optical subcarrier | [16–256] QAM |
| number of optical subcarriers | 64–256 |
| cyclic prefix | 2% |
| DFB spectral width | 0.5 nm |
| SSMF length ($L$) | 20–100 km |
| SSMF attenuation coefficient | 0.2 dB/km |
| SSMF chromatic dispersion coefficient | 17 ps/nm/km |
| APD responsivity ($R$) | 0.9 A/W |
| APD temperature ($T$) | 300 K |
| APD load charge resistance | 10 kΩ |
| APD MF | 200 |
| APD gain ($G$) | 15 |
| APD bandwidth ($\Delta F$) per optical subcarrier | 20 GHz |
| bit rate | 40–160 Gb/s |
| wavelength bandwidth ($\Delta\vartheta$) | 90 nm |
| simultaneous users | 45 |

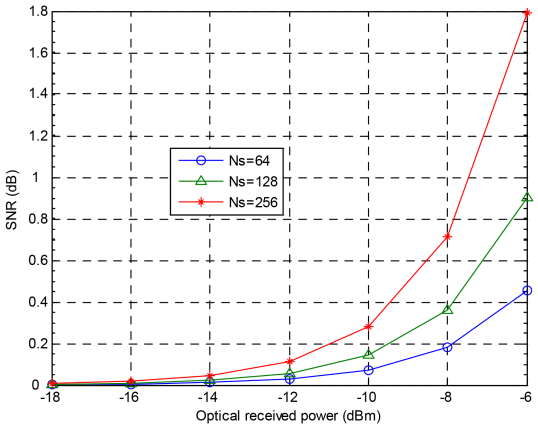


**Fig. 2** *SNR versus received power, $P_R$, of AO-OFDM-CDMA for the different numbers of optical subcarriers, $N_s$, at 40 Gb/s for transmission through 20 km and K = 45*

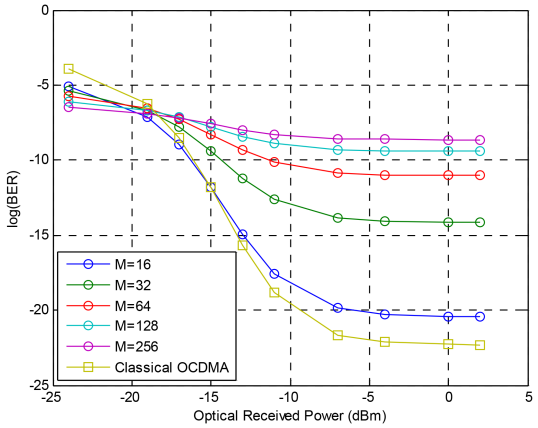


**Fig. 3** *Log(BER) versus $P_R$ for AO-OFDM-OCDMA at 40 Gb/s and compared with 'classical' WDM-OCDMA at 20 km of transmission and K = 2*

modulation formats ($M$) on $N_S$ and a comparison is made with a classical WDM-OCDMA, whose set-up and parameters are detailed in [12, 16]. For PR > −18 dBm, the BER is considerably reduced for both classical WDM-OCDMA and the proposed hybrid system at 20 km transmission and a code signature of $K = 2$. This is because for high PR, the SNR is increased by means of detected current ($I$) enhancement at the photodetector, thus resulting in BER improvement following (10). Moreover, when the SNR is considerably decreased, which is correlated to a low PR, a high $M$ results in improved BER. On the contrary, when the SNR is increased and being proportional to a high PR, a larger $M$ significantly degrades the BER. On the other hand, the WDM-OCDMA outperforms the hybrid system at PR > −18 dBm but it has worst performance slightly for low PR values. This is because in WDM-OCDMA, there is the absence of overlapping channels or optical subcarriers and $M$ is minimum (=1).

Fig. 4 illustrates the impact of 40 Gb/s on fibre length for different $M$ and is also compared with classical 40 Gb/s (per channel) WDM-OCDMA. For transmission distances up to 180 km, a lower $M$ improves the BER; however, using 16-QAM for distances >125 km, the BER is degraded. The latter occurs since in long distances the SNR gets smaller and according to (11) only a high $M$ can improve it. In comparison to the classical WDM-OCDMA, our system outperforms for any $M$ and up to 180 km. This can be explained once again by (11), where BER and $M$ are inversely proportional (i.e. when $M$ is increasing, BER is decreasing) and the classical OCDMA system always has the minimum value $M$ (=1).

In Figs. 5 and 6, the two systems under test are compared in terms of simultaneous users ($K$) per optical subcarrier and bit rate, respectively. From Fig. 5, it is evident that for >100 simultaneous users, a lower $M$ degrades the BER, while below this number of users only 16-QAM (the lowest adopted level of modulation) can improve it. This is explained by the fact that when the number of users increases, inter-subcarrier crosstalk (i.e. MAI defined as the contribution of the undesired users) degrades the code orthogonality in the desired receiver causing SNR degradation. On the other hand, when $K$ is small, 16-QAM can improve system performance since the SNR is high, while in comparison with OCDMA, our proposed approach outperforms for any number of $K$s. At this point, it is interesting to note that our hybrid solution which employs 2D-HC outperforms to the benchmark OFDM-CDMA-based upstream PON system reported in [15] which uses 1D Walsh–Hadamard codes. In [15], for a $K$ of 9 and 6 for the electronic-based OFDM signal, the BER is $1.4 \times 10^{-3}$ and $1.5 \times 10^{-4}$, respectively, whereas in our case as shown in Fig. 5 the obtained BERs are $<10^{-5}$ for up to 120 users per optical subcarrier. Fig. 6 shows that for bit rates up to 120 Gb/s per optical subcarrier the classical WDM-OCDMA outperforms to our hybrid system for $K = 2$ and 20 km of transmission. In particular, an improvement of 0.5 and 9 dB in Q-factor is observed by OCDMA when compared with 16- and 256-QAM OFDM-OCDMA, respectively. However, when 16-QAM modulation is employed for bit rates >120 Gb/s and up to 160 Gb/s, the OFDM-OCDMA system has slightly improved Q-factor.

In Fig. 7, we show simulated results over SSMF by adopting the well known non-linear Schrödinger equation in the split-step Fourier method [22, 23] including both linear (chromatic dispersion, polarisation-mode dispersion) and non-linear effects ($n2$ Kerr-induced non-linearity) for IM/DD 16-QAM AO-OFDM-CDMA and a conventional multi-channel 16-QAM optical OFDM system using coherent technology (CO-OFDM with in-phase and quadrature (IQ) modulation at transmitter and homodyne coherent receiver) with procedure identical to [23]. In summary, the WDM-CO-OFDM provides 10 GHz spacing between nine channels with 40 Gb/s signal capacity (25 GS/s sampling rate) per-channel using 16-QAM. CO-OFDM is comprised of 64 electronic subcarriers, a cyclic prefix of 2% to eliminate inter-symbol-interference, ten pilot subcarriers for carrier recovery and digital-to-analogue/analogue-to-digital converter clipping ratio and quantisation bits set at 13 dB and 10, respectively. For AO-OFDM-CDMA on this set-up also nine optical subcarriers are considered supporting 45 simultaneous users via OCDMA. The fifth middle channel is investigated in Fig. 7, which suffers the most from non-linear crosstalk effects, while the LOP per-channel/optical subcarrier was fixed at optimum 2 dBm for both cases in amplifier-free downstream LR-PON. The generated bits were $2^{19} - 1$ and hard-error decoding was performed at the receiver to calculate the BER. The lasers, MODs and related APD detector (IM/DD AO-OFDM-CDMA) and PIN photodetectors (WDM-CO-OFDM) were simulated according to [13]. The developed OFDM transceivers, as well as the optical

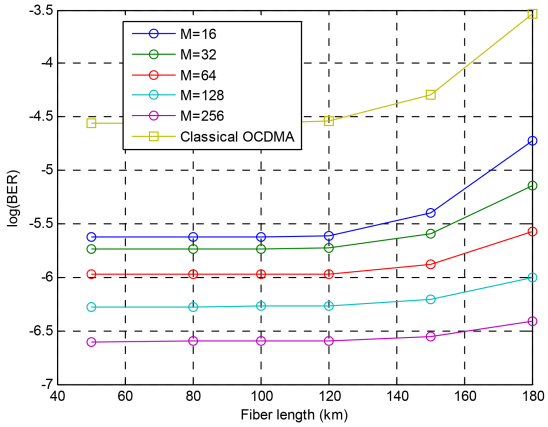


**Fig. 4** *Log(BER) versus fibre length of AO-OFDM-CDMA for 40 Gb/s and K = 45 compared with classical WDM-OCDMA*

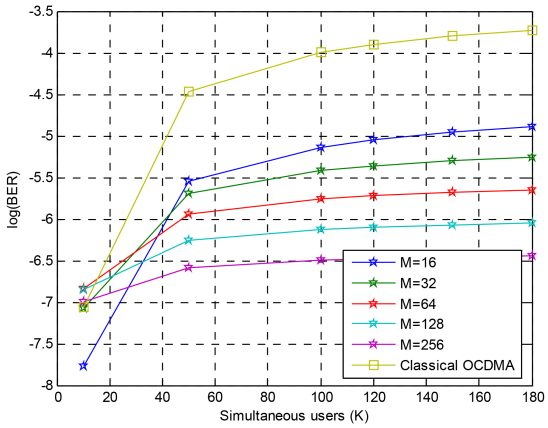


**Fig. 5** *Log(BER)versus simultaneous users (K) of AO-OFDM-CDMA at 40 Gb/s per optical subcarrier using different M and compared with classical WDM-OCDMA at 20 km of transmission*

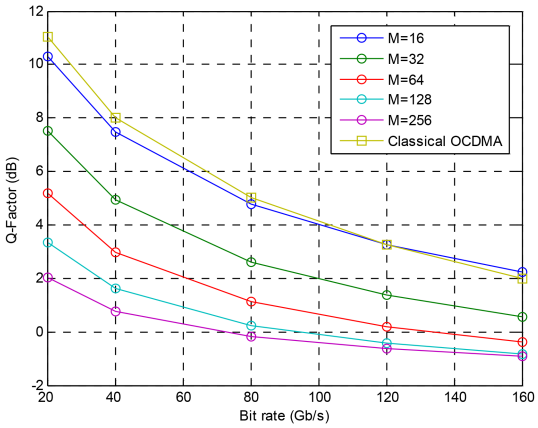


**Fig. 6** *Q-factor of OFDM-OCDMA and classical OCDMA versus bit rate at 20 km of transmission K = 2*

transmission, was implemented in a MATLAB/VPI-transmissionMaker® co-simulated environment (electrical domain in MATLAB and optical components with SSMF in VPI). It should be noted that phase noise and frequency offset has been considered here using three OFDM pilot subcarriers. Our developed system considered 1000 symbols per subcarrier. The adopted SSMF parameters in this paper for signal transmission of up to 100 km without optical amplification are as follows: fibre non-linear Kerr parameter, CD, CD slope, fibre loss and polaris-mode dispersion coefficient of 1.1 W−1 km−1, 16 ps/nm/km, 0.06 ps/km/nm2, 0.2 dB/km and 0.1 ps/km0.5, respectively. It is shown that our hybrid solution in a simple IM/DD configuration has comparable performance with WDM-CO-OFDM at the forward-error-correction limit (FEC limit) of $8 \times 10^{-3}$, which contributes to a transmission reach of 58 km (11.6 dB/km fibre loss) and 16.53 dB PON split loss (theoretical 1:45 split ratio). Above 58 km, the traditional WDM-CO-OFDM system outperforms to our hybrid solution because optical non-linear inter-subcarrier crosstalk effects (e.g. four-wave mixing, cross-phase modulation) begin to play a role in the transmission performance of AO-OFDM-CDMA. On the other hand, even though the presence of a high peak-to-average power (PAPR) ratio in WDM-CO-OFDM usually enhances the non-linear crosstalk effects, the short length of transmission and the low number of generated electronic subcarrier slower the PAPR.

In summary, as a direct result from Figs. 5 and 7, the crosstalk between different users, the increasing of the bit rate and the inter-subcarrier crosstalk are the major factors that contribute to the degradation of the AO-OFDM-CDMA system performance.

## 6 Feasibility of the proposed system

In this section, we propose the feasibility of the physical implementation of the proposed system in terms of LR-PON configuration for 45 users with 40 Gb/s bit rate. In addition, the budget calculation is performed to deduce the maximum achievable distance between OLT and ONU.

Fig. 8 shows the feasibility of the physical implementation of the proposed AO-CDMA-OFDM system in PON context in order to reach 45 users. As shown in Fig. 8, two stages of 1 × 8 couplers are employed with 64 users at full capacity (i.e. each user is using a 2D-OCDMA code as a signature). Additionally, it is convenient to select $P$ equal to 7 for 2D-HC construction sequences to reach the desired number of simultaneous users in the network. Hence, the maximum number of the constructed signature or code is equal to 56 [i.e. for 2D-HC, the total number of the generated code is proportional to $P \times (P + 1)] > 45$ simulated users.

Table 4 presents the power budget calculation related to the proposed AO-OCDMA-OFDM system configuration based on Fig. 8.

In the budget power calculation, the emitted average power of the DFB-LD and the APD photodetector sensitivity for QAM 40 G signal and standard FEC (BER = $10^{-3}$) are equal to 10 and −35 dBm, respectively [24]. For the connector attenuation, six connectors are needed in total to rely each component on the link as shown in Fig. 8 (i.e. a connector is required to connect the following components: ONU, SSMF, first coupler 1 × 8, SSMF, second coupler 1 × 8, SSMF and OLT) and if we consider that each connector has a loss of 0.4 dB [25] we get a 6 × 0.4 = 2.4 dB as the total connector attenuation in the uplink (UL). Furthermore, the entire attenuation due to the coupler is equal to 18 dB (i.e. each coupler 1 × 8 introduces a loss equal to 9 dB).

## 7 Conclusion

A novel probabilistic model for hybrid IM/DD AO-OFDM-CDMA which employs optical subcarrier hopping by means of the advanced 2D-HC signature was analysed for amplifier-free LR-PON including subcarrier overlapping, MAI and receiver beat noise. The performance of AO-OFDM-CDMA for the upstream direction at 40 Gb/s supporting 45 users at 20 km of transmission was enhanced at high optical received powers (PR) and a number of subcarriers. When SNR was small, a high modulation format ($M$) improved the BER for more than 40 and up to 180 simultaneous users; however, below 40 users 16-QAM had a definite benefit. On the other hand, at 40 Gb/s, the lowest $M$ achieved the best BER for up to 180 km. In comparison to the 'classical' WDM-OCDMA, our hybrid solution at 40 Gb/s outperformed for any number of users and distances at low PR. On the contrary, using 16-QAM in AO-OFDM-CDMA, the transmission performance was improved only at bit rates higher than 120 Gb/s. It was also shown that in comparison with conventional 1D Walsh–Hadamard, 1D-PC and 2D-PHS, coding with 2D-HC could improve the performance of our hybrid solution, thus enabling a higher number of simultaneous users. Finally, from numerical simulations where we considered both linear and non-linear effects, it was shown that 16-QAM AO-OFDM-CDMA with

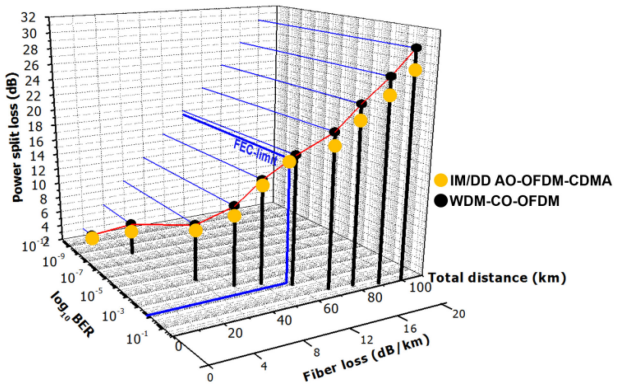


**Fig. 7** *Comparison of simulated IM/DD AO-OFDM-CDMA (K = 45) and WDM-CO-OFDM in downstream amplifier-free LR-PON for 16-QAM: log(BER) versus distance providing the power split loss and fibre loss for each value*

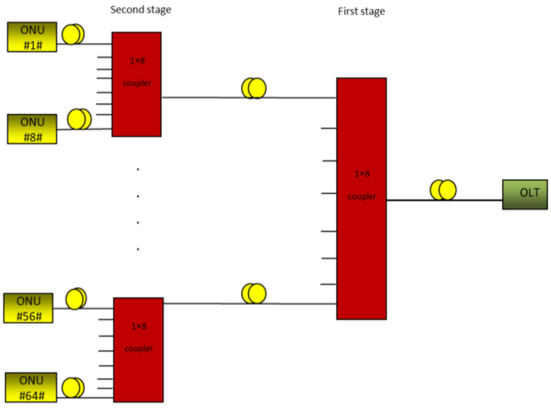


**Fig. 8** *Feasibility implementation of the upstream AO-OCDMA-OFDM system*

**Table 4** Power budget calculation

| Parameter, unit | Value |
|---|---|
| emitted average power, dBm | 10 |
| connectors attenuation, dB | 2.4 |
| coupler attenuation, dB | 18 |
| system margin, dB | 3 |
| received average power, dBm | −35 |
| $a$ = available attenuation, dB | 21.6 |
| maximal distance between ONU and OLT ($a/\alpha$), km | 108 |

45 users has comparable performance with conventional WDM-CO-OFDM in the downstream direction for up to 58 km and 1:45 split ratio, without employing complex and energy-demanding coherent technology.

## 8 Acknowledgments

The work of Dr. Elias Giacoumidis was emanated from EU Horizon 2020 research and innovation programme under the Marie Skłodowska-Curie Grant agreement no. 713567 and in part by a research grant from Science Foundation Ireland (SFI) and is co-funded under the European Regional Development Fund under Grant No. 13/RC/2077.

## 9 References

[1] Subramanian, M.: '*Network management, principles and practice*' (Pearson Edition, Chennai, 2010)

[2] Shaukat, S.F., Ibrahim, U., Nazir, S.: 'Monte Carlo analysis of broadband passive optical networks', *World Appl. Sci. J.*, 2011, **12**, (8), pp. 1156–1164

[3] Kramer, G., Mukherjee, B., Pesavento, G.: 'Ethernet PON (ePON): design and analysis of an optical access network', *Photonics Netw. Commun.*, 2001, **3**, (3), pp. 307–319

[4] Ragheb, M., Elnamaky, M., Fathallah, H., *et al.*: 'Performance evaluation of standard IPACT for future long reach passive optical networks (LR-PON)'. Proc. Int. Conf. Communication Technologies, Riyadh, Saudi Arabia, 2010

[5] 10-Gigabit-capable passive optical network (XG-PON) systems, ITU-T Recommendation G987

[6] Muciaccia, T., Gargano, F., Passaro, V.M.N.: 'Passive optical access networks: state of the art and future evolution', *IEEE Photonics J.*, 2014, **1**, pp. 323–346

[7] Hillerkuss, D., Schmogrow, R., Schellinger, T., *et al.*: '26 tbit $s^{-1}$ line-rate super-channel transmission utilizing all-optical fast Fourier transform processing', *Nat. Photonics*, 2011, **5**, pp. 364–371

[8] Chow, C., Yeh, C., Sung, J., *et al.*: 'Direct-detection all-optical OFDM superchannel for long-reach PON'. Proc. 13th IEEE Int. Conf. Optical Communications and Networks (ICOCN), Suzhou, China, November 2014

[9] Giacoumidis, E., Wei, J.L., Yang, X.L., *et al.*: 'Adaptive-modulation-enabled WDM impairment reduction in multichannel optical OFDM transmission systems for next-generation PONs', *IEEE Photonics J.*, 2010, **2**, (2), pp. 130–140

[10] Mao, T., Wang, Z., Wang, Q., *et al.*: 'Dual-mode index modulation aided OFDM', *IEEE Access J.*, 2017, **5**, pp. 23871–23880

[11] Wong, E.: 'Next-generation broadband access networks and technologies', *IEEE J. Lightwave Technol.*, 2012, **30**, (4), pp. 597–608

[12] Mrabet, H., Dayoub, I., Attia, R.: 'A comparative study of 2D-OCDMA-WDM system performance in 40G-PON context', *IET Optoelectron.*, 2017, **11**, (4), pp. 141–147

[13] Wang, X., Gao, Z., Wang, X., *et al.*: 'Bit-by-bit optical code scrambling technique for secure optical communication', *OSA Opt. Express*, 2011, **19**, (4), pp. 3503–3512

[14] Mhatli, S., Mrabet, H., Giacoumidis, E., *et al.*: 'Performance evaluation of an IMDD optical OFDM-CDMA system', *Appl. Opt.*, 2018, **57**, (7), pp. 1569–1574

[15] van Veen, D.T., Houtsma, V.E., Gnauck, A.H., *et al.*: 'Demonstration of 40 Gb/s TDM-PON over 42 km with 31 dB optical power budget using an APD-based receiver', *IEEE J. Lightwave Technol.*, 2015, **33**, (8), pp. 1675–1680

[16] Mrabet, H., Dayoub, I., Attia, R., *et al.*: 'Performance improving OCDMA system using 2-D optical codes with optical SIC receiver', *IEEE J. Lightwave Technol.*, 2009, **27**, (21), pp. 4744–4753

[17] Mrabet, H., Attia, R., Dayoub, I.: 'Analysis of the error probability for optical unipolar two-dimensional codes using a serial elimination interferences receiver'. 2007 ICTON Mediterranean Winter Conf. (ICTON-MW), Sousse, Tunisia, 6–8 December 2007, pp. 1–4

[18] Majumder, S., Azhari, A., Abbou, F.: 'Impact of fiber chromatic dispersion on the BER performance of an optical CDMA IM/DD transmission system', *IEEE Photonics Technol. Lett.*, 2005, **17**, (6), pp. 1340–1342

[19] Agrawal, G.: '*Fiber-optic communications systems*' (Wiley-Interscience publication, 2012, 5th edn.)

[20] 'Characteristics of a single-mode optical fibre and cable', Recommendation ITU-T G.652, 2009

[21] Guo, X., Wang, Q., Zhou, L., *et al.*: 'High-speed OFDM-CDMA optical access network', *OSA Opt. Lett.*, 2016, **41**, (8), pp. 1809–1812

[22] Agrawal, G.P.: '*Nonlinear fiber optics*' (Academic Press, Cambridge, MA, 2012, 5th edn.)

[23] Giacoumidis, E., Jarajreh, M.A., Sygletos, S., *et al.*: 'Dual-polarization multi-band OFDM transmission and transceiver limitations for up to 500 Gb/s in uncompensated long-haul links', *OSA Opt. Express*, 2014, **22**, (9), pp. 10975–10986

[24] 'Assessment of advanced LR-PON transmission schema', DISCUS Consortium, 2013

[25] Brown, G., Creath, K., Kogelnik, H., *et al.*: '*The optics encyclopedia (basic foundations and practical applications)*' (Wiley, Hoboken, 2004)